Chemical Engineering Journal 155 (2009) 419–426

Contents lists available at ScienceDirect

Chemical Engineering Journal

journal homepage: www.elsevier.com/locate/cej

Modeling and simulation of a smart catalytic converter combining NOx storage, ammonia production and SCR

R. Zukerman[a], L. Vradman[a], M. Herskowitz[a,*], E. Liverts[a], M. Liverts[a], A. Massner[b], M. Weibel[b], J.F. Brilhac[c], P.G. Blakeman[d], L.J. Peace[d]

[a] Blechner Center for Industrial Catalysis and Process Development, Department of Chemical Engineering, Ben-Gurion University of the Negev, Beer-Sheva 84105, Israel
[b] Daimler AG, Mercedesstrasse 137, 70546 Stuttgart, Germany
[c] Laboratoire Gestion des Risques et Environnement, Universite' de Haute-Alsace, France
[d] Johnson Matthey Environmental Catalysts and Technologies, European Technology Centre, UK

ARTICLE INFO

Article history:
Received 19 June 2009
Received in revised form 31 July 2009
Accepted 16 August 2009

Keywords:
Catalytic converter
Simulation
NOx storage
Ammonia production
Selective catalytic reduction

ABSTRACT

Dynamic simulation of the smart catalytic converter, proposed by Daimler AG, is presented. The smart catalytic converter combines NOx storage, on-board ammonia production and selective catalytic reduction (SCR) and functions in a dual-mode operation, alternating between lean burn and rich burn. It relies on intrinsic dynamic operation and synchronization of all units and its development demands a reliable dynamic simulator. A platform capable of simulating the dynamic behavior of multiple-unit aftertreatment system was developed based on COMSOL package. Predictive kinetic models were developed for NOx storage unit that includes ammonia formation function and for NH_3-SCR unit. Using these kinetic models, two-unit smart catalytic converter was simulated on the developed simulator. The results of the simulator were validated using two-unit experimental data. The simulator was also employed to control and optimize the performance of smart catalytic converter. It was shown that the simulator is vital for optimization of lean and rich periods in order to ensure stable lean–rich cycles.

© 2009 Elsevier B.V. All rights reserved.

1. Introduction

Development of lean burn engines running with excess air is aimed at reducing fuel consumption and greenhouse gas emissions [1]. However, lean engines increase significantly NOx emission thus creating a major environmental and health problem [2,3]. Traditional aftertreatment systems based on the three-way catalyst (TWC) display poor performance under oxygen excess [4,5]. This led to develop novel technologies of NOx removal for a lean burn engines, including catalytic NOx decomposition [6], NOx storage reduction (NSR) [7,8] and selective catalytic reduction (SCR) by ammonia [9,10] or hydrocarbons [6]. Over the last decade, the worldwide emission legislation has become increasingly stringent [11]. Therefore, the exhaust aftertreatment systems need to be modified to comply with new emission regulation. Combined aftertreatment systems, consisting of different catalysts are being developed. The BlueTec system, developed by Daimler AG, consists of diesel oxidation catalyst (DOC), diesel particulate filter (DPF), NSR and SCR catalysts [12]. Researchers at Ford also proposed combined aftertreatment system consisting of DOC, NH_3-SCR and a catalyzed DPF [13]. The DOC unit is applied to oxidize the unburned hydrocarbons (HCs), CO and NO and raise the exhaust temperature for active regeneration of DPF, while the latter was used for controlling the particulate matter (PM). The SCR unit is employed to reduce the NOx by NH_3 supplied from an externally source. Combining the NH_3 production and NH_3-SCR units were proposed by Qgunwumi et al. [14] to eliminate the need for an ammonia source. Ammonia is produced by the reaction between NOx from the exhaust gas and injected reductant agent. Combined aftertreatment system consisting of HCs trap and TWC was proposed for cold start [5]. Other combined aftertreatment systems have been proposed as NOx storage with TWC [15], DOC with NH_3-SCR [12,16].

The smart catalytic converter system was first proposed in 2002 by Guenther et al. [17]. This system combines two technologies for NOx removal in lean burn engines: NOx storage and NH_3-SCR with on-board NH_3 production. The system functions in a dual-mode operation, alternating between lean and rich modes. During the lean mode, NOx is partially stored in the NOx storage unit, while the rest continues to the NH_3-SCR unit where it reacts with adsorbed NH_3 to form N_2. During the rich operation, NOx is desorbed from the NOx storage unit and reacts with hydrogen and/or other reductants in the ammonia production unit to form ammonia, subsequently adsorbed in the NH_3-SCR unit. This enables a cycled operation. The smart catalytic converter eliminates the need for an external

* Corresponding author. Tel.: +972 8 6472421; fax: +972 8 6477745.
E-mail address: herskow@bgu.ac.il (M. Herskowitz).

1385-8947/$ – see front matter © 2009 Elsevier B.V. All rights reserved.
doi:10.1016/j.cej.2009.08.015

Nomenclature

a_v	gas solid interfacial area per unit reactor volume ($m^2_{solid}\, m^{-3}_{reactor}$)
c_{pg}	gas phase heat capacity ($J\, kg^{-1}_{gas}\, K^{-1}$)
c_{ps}	solid phase heat capacity ($J\, kg^{-1}_{solid}\, K^{-1}$)
C_t	overall molar concentration of gas phase ($kmol_{total}\, m^{-3}_{gas}$)
$(-\Delta H)_i$	heat of reaction i ($J\, kmol^{-1}$)
k_i	reaction rate constant ($kmol\, kg^{-1}_{cat}\, s^{-1}$)
k_h	heat transfer coefficient ($J\, m^{-2}_{solid}\, K^{-1}\, s^{-1}$)
k_m	mass transfer coefficient ($kmol\, m^{-2}_{solid}\, atm^{-1}\, s^{-1}$)
K_j	adsorption constant of component j
L	monolith length (m)
M_m	mean molecular mass of gas phase ($kg_{gas}\, kmol^{-1}_{gas}$)
P_t	overall gas pressure (atm)
r_i	rate of reaction i ($kmol\, kg^{-1}_{cat}\, s^{-1}$)
t	time (s)
T_g	gas phase temperature (K)
T_s	solid phase temperature (K)
u_s	superficial gas velocity ($m^3_{gas}\, m^{-2}_{reactor}\, s^{-1}$)
y_g	component mole fractionate bulk gas phase ($kmol_j\, kmol^{-1}_{total}$)
y_s	component mole fractionate gas phase near solid surface ($kmol_j\, kmol^{-1}_{total}$)
z	reactor axial coordinate (m)

Greek letters

Ω	catalyst adsorption capacity for NO or NH_3 ($kmol_j\, kg^{-1}_{cat}$)
α_{ji}	stoichiometric coefficient of component j in the ith reaction
ε_b	monolith void fraction ($m^3_{gas}\, m^{-3}_{reactor}$)
θ_j	jth component surface coverage fraction
λ_s	solid thermal conductivity ($J\, m^{-1}_{solid}\, K^{-1}_{reactor}\, S^{-1}$)
ρ_b	catalyst bulk density ($kg_{cat}\, m^{-3}_{reactor}$)
ρ_g	gas density ($kg_{gas}\, m^{-3}_{gas}$)
ρ_s	solid bulk density ($kg_{solid}\, m^{-3}_{reactor}$)

Subscripts

ads	adsorption
cat	catalyst
g	gas phase
i	reaction number
j	component index
s	solid phase

reductant, such as urea or ammonia. Furthermore, the NOx storage unit volume in this configuration is smaller than conventional NOx storage units, reducing cost of precious metal.

Recently, the concept of the smart catalytic converter was experimentally tested over double-bed reactor: NSR (Pt-Ba/Al_2O_3 catalyst) and SCR (Fe-ZSM5) [18]. Ammonia released from NSR catalyst during rich mode can be stored on the SCR catalyst, while in the lean mode the stored ammonia can react with NOx. The SCR catalyst bed placed downstream of the NSR reduces the NH_3 slip and increases the NOx removal efficiency [18]. This system relies on intrinsic dynamic operation and synchronization of all units. In addition, it renders the units integration and precise scheduling necessary to achieve the desired performance. Thus, it is necessary to develop dynamic models that simulate the system performance providing the tools for dynamic control.

Mathematical modeling of catalytic converter systems was applied in the design, control and optimization of aftertreatment systems. Over the past three decades, numerous mathematical models of catalytic converters were developed at different complexity levels for a range of applications [12,19,20]. The kinetic models were derived from both fundamental [21–24] and semi-empirical studies [25–28]. Fundamental models require the evaluation of a large number of kinetic parameters from detailed kinetic data over a wide range of conditions and configurations. Furthermore, they are specific for well-defined catalytic systems. This is very difficult to accomplish. Therefore, most kinetic models for the catalytic converter are semi-empirical.

The reactor model combines transport and kinetic models of the catalytic converter, expressed in mass and heat differential balances for the gas and solid phases. The pressure drop is normally negligible [12,20]. Simplifying assumptions are normally made without compromising the reliability of the reactor model. Axial diffusion in mass and heat transfer of the gas phase is neglected [12,29,30]. Radiation is negligible at the temperature range of interest [20,30,31]. Plug flow and ideal gas behavior are acceptable, while all channels are assumed to be identical [12,26,30]. In addition, any effects of pore diffusion through the washcoat are lumped in the kinetic parameters [20]. Most models are one-dimensional [19,20,26,29,30,32–36] rather than more complex models [35,37–40] which normally present little advantage. A quasi-steady state is normally assumed, neglecting the accumulation term in the gas phase [20,30,38]. This is not valid for the smart catalytic converter that operates in a dynamic mode [20].

Most of the dynamic and pseudo-steady state simulations that have been published in the literature, deal with single-unit catalytic converters [19,20,22–24,26–30,32–36]. Lately, several simulation programs have been developed for combined systems [12,13,16,41]. A software environment called ExACT has been developed by Daimler AG [12]. The software is based on Matlab/Simulink and includes models for different types of catalysts and particulates filter, such as, TWC, NSR, SCR and coated DPF [12,41]. Simulations of combined aftertreatment system based on DOC and urea-SCR unit have also been undertaken by Wurzenberger and Wanker [16]. 1D model with global kinetic reaction was employed to simulate this system. Other simulation programs for aftertreatment systems are GT-POWER and AMESim [12]. These programs include models for engine components as well as templates for TWC, NSR and SCR.

The model presented in this communication was developed within the framework of AHEDAT (Advanced Heavy Duty Engine Aftertreatment Technology) project [42]. The main scope was to develop a platform aimed at simulating the dynamic behavior of multiple-unit aftertreatment systems. Predictive kinetic models were developed for NOx storage unit that included ammonia formation and for NH_3-SCR. A two-unit catalytic converter (NOx storage with ammonia formation and NH_3-SCR) was simulated based on a COMSOL package. The results were compared with data from a two-unit experimental unit. The simulator was also employed to control and optimize the performance of the smart catalytic converter.

2. Experimental

2.1. Catalytic tests

Investigations of the NOx storage and NH_3-SCR (separately and of the combined system) were carried out using a test rig specially designed for testing monolith catalyst samples. The test rig included two individual gas lines enabling the step change

Table 1
The inlet gas composition of catalytic tests.

Exp.	Inlet mole fraction (vol%) (balanced with 8% H_2O and N_2)										
	Lean mode				Rich mode						
	NO	O_2	C_3H_6	CO_2	NO	O_2	H_2	C_3H_6	CO	NH_3	CO_2
EC1					0.05	1.6	1.4	0.3	4.2		11.5
EC2	0.05	8	0	8	0	1.2	1.5	0.4	4.6	0	11.3
EC3					0.05	1.6	1.4	0.3	4.2		11.5
EC4											
EC5	0.05	5	0.005	8	0	0.7	1	0.28	3	0.075	11
EC6											
EC7											

between lean and rich gas mixtures with high accuracy. The synthetic exhaust gas mixtures were dosed by a synthetic gas supply with mass flow controllers. This test rig simulated lean/rich cycles with different phase durations. The gas composition was analyzed by IR, flame ionization and chemiluminescence and mass spectrometer for NH_3.

A NOx storage catalyst in a monolith form (diameter = 17 mm, length = 55 mm) was tested at isothermal conditions. Several experiments at over a range of conditions (GHSV, temperature and gas composition) were performed (Tables 1 and 2). Two kinds of tests were done: NO adsorption during the lean period and NO desorption with ammonia formation during the rich period. First, a lean mixture (Tables 1 and 2) was fed through a bypass for 100 s. Then it was directed through the catalyst in the adsorption (loading) stage. The exhaust gas was switched to a rich mixture (Tables 1 and 2, EC1–EC3) and fed through the catalyst (the desorption stage). Before each experiment, the catalyst samples were pretreated at 500 °C under lean–rich cycle.

A monolith NH_3-SCR catalyst (19 mm diameter, 25 mm length) was tested at 212, 268, 296 and 354 °C and GHSV of 50,000 h^{-1}. Two kinds of tests were performed: NH_3 adsorption during the rich period and NO reduction during the lean period. A rich mixture (EC4–EC7, Tables 1 and 2) was fed through a bypass for 100 s, then through the catalyst in the ammonia adsorption (loading) stage. After 2 min in the bypass, the exhaust gas was switched to a lean mixture (EC4–EC7, Tables 1 and 2) and fed through the catalyst for 300 s (the NO reduction stage). At each temperature, five experiments were done at different NH_3 loading periods (10, 20, 60, 200 and 400 s). Before each experiment, SCR unit was exposed to NO/NO_2 gas mixture to consume the remaining ammonia.

The NO conversion was calculated as the difference between the total number of moles of NO at the inlet and the outlet of a particular unit divided by the total number of moles at the inlet. The total number of moles was calculated by integrating the molar flow rate of NO over the time of the lean mode or lean–rich cycle. The ammonia yield is the ratio between NH_3 that was formed during rich mode to the NO that was adsorbed during lean mode in the NOx storage unit. The ammonia slip was calculated dividing the total mole fraction of ammonia at the outlet to that at the inlet of SCR unit.

Table 2
The experimental conditions of catalytic tests.

Exp.	GHSV (h^{-1})	Temperature (°C)	Lean period (s)	Rich period (s)
EC1	37,500	240	165	7
EC2	48,750	300	233	10
EC3	60,000	375	165	7
EC4	50,000	212	300	10, 20, 60, 200, 400
EC5		268		
EC6		296		
EC7		354		

2.2. Catalytic converter model

A transient, one-dimensional, heterogeneous model of monolith channels was employed to simulate the performance of the aftertreatment system [33]. It assumes: adiabatic conditions, ideal gas phase, constant pressure and no homogenous reactions. Any mass transfer effects in the washcoat are lumped in the kinetic parameters. Correlations for external heat and mass transfer coefficients, available in the literature [43,44], were implemented in all units. Mass balances in the gas included accumulation, convection and external mass transfer. Mass balances in the solid included accumulation, external mass transfer and catalytic reactions. Heat balance in the gas included accumulation, convection and gas–solid heat transfer. Heat balance of the solid included accumulation, axial heat conduction, gas–solid heat transfer and heat generated by the reactions. Mass balances for the active sites included accumulation and catalytic reactions.

Mass balances:

$$\text{gas phase}: \frac{\varepsilon_b \rho_g}{M_m}\frac{\partial y_{g_j}}{\partial t} = -\frac{u_s \rho_g}{M_m}\frac{\partial y_{g_j}}{\partial z} - k_m a_v P_t (y_{g_j} - y_{s_j}) \quad (1)$$

$$\text{solid phase}: \varepsilon_b C_t \frac{\partial y_{s_j}}{\partial t} = k_m a_v P_t (y_{g_j} - y_{s_j}) + \rho_b \sum_{i=1}^{n} (\alpha_{ji} r_i) \quad (2)$$

Heat balances:

$$\text{gas phase}: \frac{\rho_g}{M_m} c_{pg} \varepsilon_b \frac{\partial T_g}{\partial t} = -u_s \frac{\rho_g}{M_m} c_{pg} \frac{\partial T_g}{\partial z} + k_h a_v (T_s - T_g) \quad (3)$$

$$\text{solid phase}: \rho_s c_{ps} \frac{\partial T_s}{\partial t} = (1-\varepsilon_b)\lambda_s \frac{\partial^2 T_s}{\partial z^2} - k_h a_v (T_s - T_g) + \rho_b \sum_{i=1}^{n} ((-\Delta H)_i r_i) \quad (4)$$

Active sites balance

$$\Omega \frac{d\theta_j}{dt} = \sum_{i=1}^{n} (\alpha_{ji} r_i) \quad (5)$$

The initial and boundary conditions at the inlet and outlet were expressed as:

$t = 0$: $y_{g,j}(z) = y_s(z) = y_{j_0}$; $T_g(z) = T_s(z) = T_0$(exhaust gas temperature); $\theta(Z) = \theta_0$

$z = 0$: $y_{g,j}\big|_{\text{at the first unit}} = y_{j_0}$; $y_{g,j}\big|_{\text{at the following unit}} = y_{g,j}\big|_{z=L,\ \text{at the previous unit}}$; $T_g\big|_{\text{at the first unit}} = T_0$ (exhaust gas temperature); $T_g\big|_{\text{at the following unit}} = T_g\big|_{z=L,\ \text{at the previous unit}}$

$z = L$: $\partial T_s / \partial z = 0$

The initial and inlet temperature and composition in the gas and solid phases are assumed to be the temperature and composition of the exhaust feed gas, respectively. The gas phase temperature and the composition at the inlet of each unit (but not the first unit) are assumed to be that at the outlet of the previous unit.

2.3. Modeling and simulation tools

The software package Athena Visual Workbench software (Stewart and Associates Engineering Software, Inc.) was used for numerical integration of partial differential equations (PDE) as well as for parameter estimation of the kinetic model for NH_3-SCR and the NOx storage unit. The parameter estimation was done by employing the method of least squares, whereas the best fit is approached by minimizing the sum of the squares of the offsets (residuals) between experimental values and values predicted by the model.

Commercial software COMSOL 3.2 was used for the simulation of the catalytic converter performance. The COMSOL simulator was tested with simple cases for which the solution is known, such as the case of a steady state model, an isothermal model, zero reaction rates and so on. In all case COMSOL yields similar to those of other simulation programs such as ACSL 1.3.2 (Advanced Continuous Simulation Language) and POLYMATH 6.10. In addition, for the more complicated cases (transient mode), simulation results from COMSOL and Athena programs were compared yielding similar results.

3. Results and discussion

3.1. Kinetic model for NOx storage with NH_3 production and NH_3-SCR unit

A simplified kinetic model for NOx storage unit over a commercial catalyst was developed. The kinetic parameters for the NO adsorption–desorption were estimated from the lean mode and for ammonia and nitrogen formation from rich mode data. The kinetic model for the lean mode (reactions (6) and (7), Table 3) is based on reversible adsorption and desorption of NO on the active sites [45]. The NOx storage model in the rich mode consists of four reactions: enhanced NO desorption by hydrogen, formation of ammonia and nitrogen and oxidation of ammonia (reactions (8)–(11), Table 3). The NO desorption reflects the fast NO desorption from active sites in the rich mode. Similar phenomenon was observed for Pt/HPW after addition of H_2 to the rich gas mixture containing CO and water [46] which enhanced the desorption–reduction rate of NO. It was assumed that during each lean–rich cycle, NO adsorbed in the lean mode desorbs completely in the rich mode so the concentration of formed N_2 was calculated from the N-atom balance: $NO_{adsorbed} = NO_{desorbed} + NH_{3,formed} + 0.5N_{2,formed}$. The kinetic rate expressions for ammonia and nitrogen formation were derived based on information for NO–H_2 reactions on noble metals [47–49]. Experimental data indicated that ammonia was formed only between 240 and 300 °C. At 375 °C the gas mixtures at the outlet of the storage unit did not contain ammonia, probably due to complete oxidation to nitrogen [50]. Thus, oxidation reaction of ammonia to N_2 was modeled with simple power law rate (reaction (11), Table 3). The kinetic parameters for six expressions of the NOx storage unit model in the lean and rich modes were estimated from kinetic data using the Athena Visual software.

Table 3
Kinetic model of the NOx storage unit.

Reaction		Expression
$site + 2NO \xrightarrow{r_1} (NO)_{2,ads}$	(6)	$r_1 = k_1 P_t(1-\theta_{NO})(y_{NO})$
$(NO)_{2,ads} \xrightarrow{r_2} site + 2NO$	(7)	$r_2 = k_2\theta_{NO}$
$(NO)_{2,ads} + H_2 \xrightarrow{r_3} site + 2NO + H_2$	(8)	$r_3 = k_3 P_t \theta_{NO} y_{H_2}$
$NO + \frac{3}{2}H_2 \xrightarrow{r_4} NH_3 + H_2O$	(9)	$r_4 = \frac{k_4 P_t^2 y_{NO} y_{H_2}}{(1+K_4 P_t y_{NH_3})^2}$
$NO + H_2 \xrightarrow{r_5} \frac{1}{2}N_2 + H_2O$	(10)	$r_5 = \frac{k_5 P_t y_{NO}}{1+K_5 P_t y_{NO}}$
$NH_3 + O_2 \xrightarrow{r_6} \frac{1}{2}N_2 + H_2O$	(11)	$r_6 = k_6 P_t y_{NH_3}$

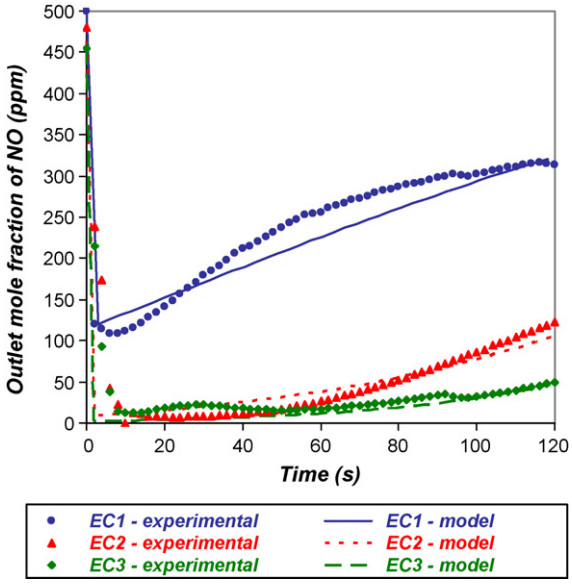

Fig. 1. Data fit by the model for NO adsorption in the NOx storage unit in the lean mode.

The good fit of experimental NO data during the lean mode at various conditions (EC1–EC3) is illustrated in Fig. 1. Fig. 2A shows a good agreement between calculated and experimental NO and NH_3 concentrations during the lean and rich modes at EC1 condition. The model also predicts the ammonia yields and the total NO conversion for one lean–rich cycle (Fig. 2B). Furthermore, the model was validated using separate experiments that were not included in the fitting process (200–550 °C, 60,000 h^{-1}, 600 ppm NO in the feed). The results predicted by the model indicated good agreement with the experimental data.

The kinetic model for SCR reaction in the NH_3-SCR unit over a commercial catalyst consists of three reactions: NO reduction (reaction (14), Table 4), ammonia adsorption and desorption (reactions (12) and (13), Table 4). The kinetic model assumed a Temkin-type kinetic expression for the local rates of ammonia desorption [51]. It takes into account the catalyst surface heterogeneity in agreement with the physico-chemical characterization of the catalysts [52,53]. Ammonia oxidation was not taken into account since oxidation of ammonia is significant only at high temperature (≥350 °C) [54].

Fig. 3 depicts the outlet mole fraction of NO and NH_3 at EC5 conditions. During the lean and rich mode, the data fit is good. The deviation at the start of rich mode is probably caused by the bypass used in the experiments. Similarly, good data fit for the outlet mole fraction of NO and ammonia was achieved for other conditions – EC4, EC6 and EC7. Fig. 3 also shows the good agreement between experimental and model results for amount of adsorbed ammonia normalized to the catalyst adsorption capacity (θ_{NH_3}) during the rich and lean period. Good agreement between calculated and experimental NO conversion during the lean mode (300 s) after 60 s in the rich mode was obtained for EC4–EC6 conditions (Fig. 4). The little deviation between the experimental and calculated NO con-

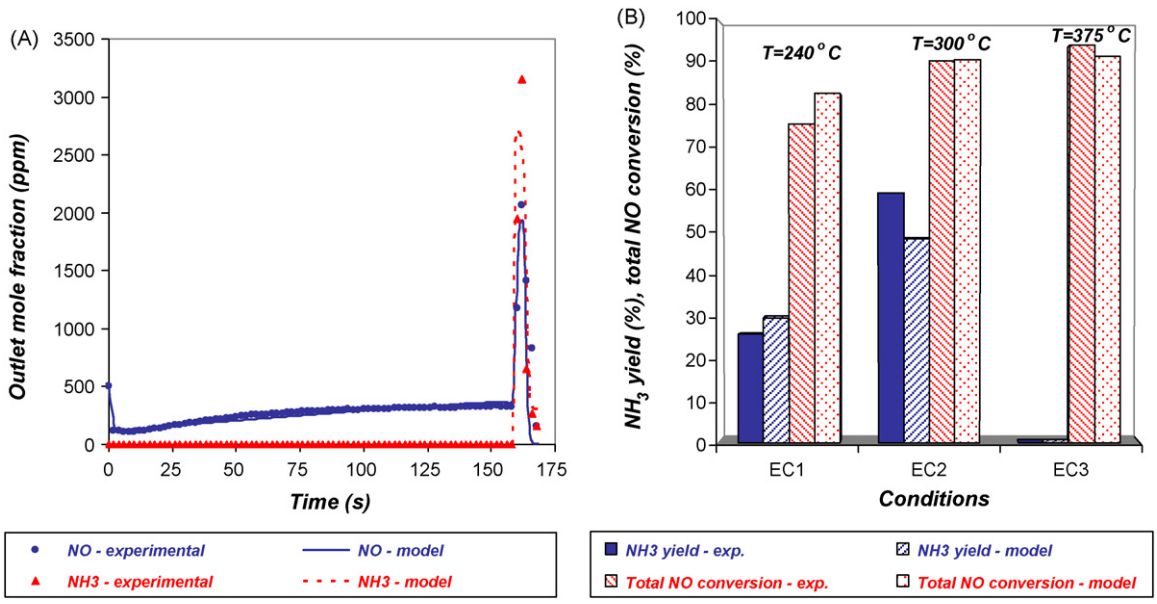

Fig. 2. (A) Data fit by the kinetic model for NO and ammonia outlet concentration in the NOx storage unit during the rich and lean modes. Condition: EC1. (B) Experimental and calculated ammonia yield during the rich mode and overall NO conversion in the NOx storage unit.

version at EC7 is probably due to the oxidation of ammonia. Above 350 °C, part some ammonia reacts in side reactions, leaving less ammonia to react with NO in SCR reaction. It decreased the NOx conversion above 350 °C [54] Thus, the proposed model provides a good description of the NH_3-SCR performance under transient conditions below 350 °C.

Table 4
Kinetic model of the NH_3-SCR unit.

Reaction		Expression
$NH_{3,g} \xrightarrow{r7} NH_{3,ads}$	(12)	$r_7 = k_7(1-\theta_{NH_3})y_{NH_3}$
$NH_{3,ads} \xrightarrow{r8} NH_{3,g}$	(13)	$r_8 = k_8\theta_{NH_3}$
$4NO + 4NH_{3,ads} + O_2 \xrightarrow{r9} 4N_2 + 6H_2O$	(14)	$r_9 = k_9 y_{NO}\theta_{NH_3}$

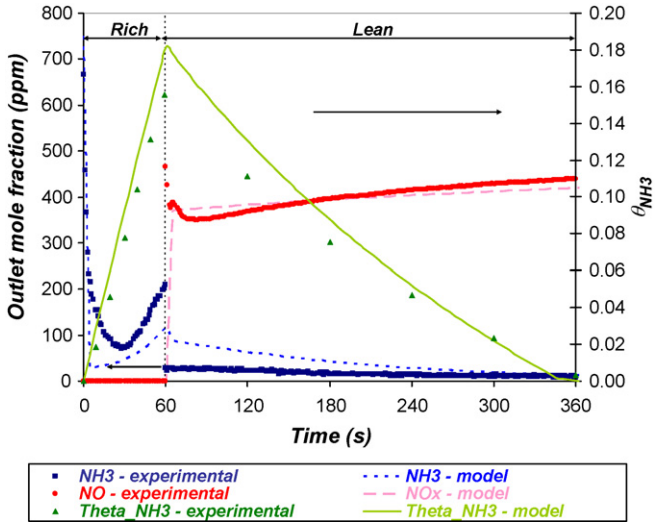

Fig. 3. Data fit by the NH_3-SCR model. Condition: EC5.

3.2. Simulation of the two-unit integrated system (NO storage and NH_3-SCR units)

The kinetic models of the individual units were used for simulating the two-units integrated system. Transient mass balances in the gas and solid in the two units (NOx storage and NH_3-SCR) were solved simultaneously. The different size and characteristic time scale of each unit render the numerical solution complex.

Fig. 5 displays a good agreement of NO in NOx storage and NH_3-SCR units (lean and rich mode at EC1). The model also predicts the NO conversion and NH_3 slip (the ratio between the accumulated mole fraction of NH_3 at the inlet and outlet of SCR unit) (Fig. 6). Similar results were achieved at EC2. The kinetic models of the NOx storage and NH_3-SCR were developed based solely on the experiments with the individual units. No additional data fit was performed.

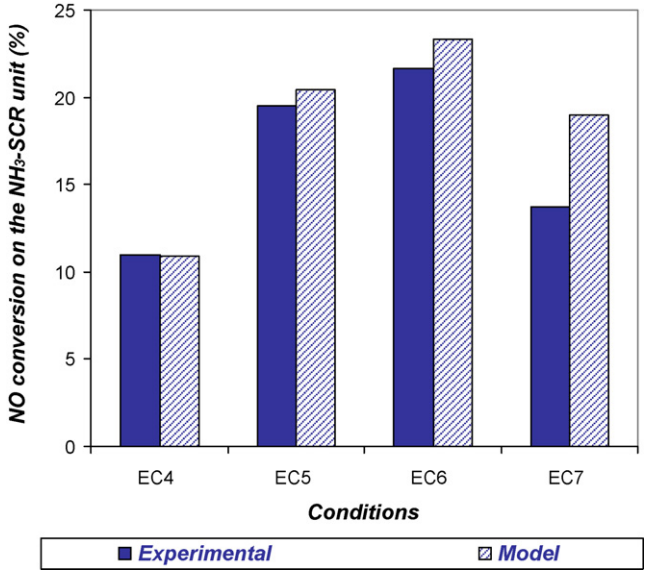

Fig. 4. Experimental and calculated NO conversion in NH_3-SCR at lean mode at several conditions (EC4–EC7); rich mode, 60 s; lean mode, 300 s.

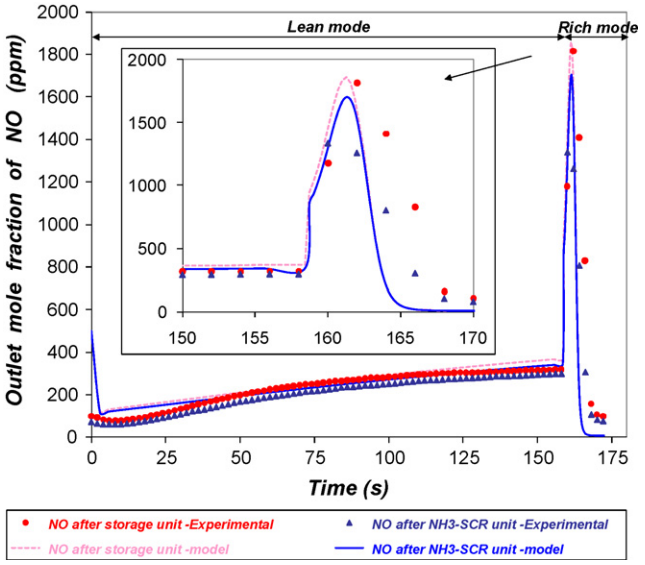

Fig. 5. Prediction of the outlet NO mole fraction from storage and NH_3-SCR units at EC1.

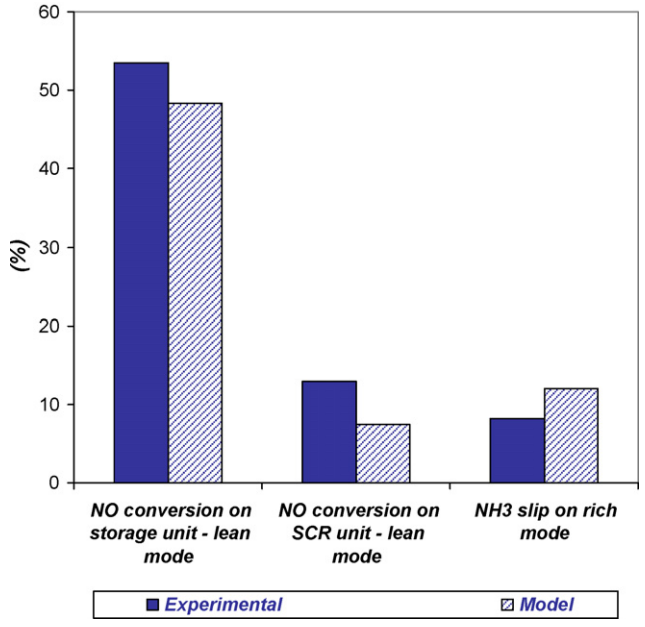

Fig. 6. Prediction of the two-unit integrated system performance at EC1.

The simulator of the integrated system is very useful for system optimization and control. The key factor for the aftertreatment system stability and control is the balance between adsorbed and desorbed NO in the storage unit. In addition, the amount of NH_3 reacted during the lean period in SCR unit should be balanced by the NH_3 production in storage unit during the rich period. This ensures stable lean–rich cycles. Results from the simulation demonstrated that the experimental time periods for rich and lean mode at EC1 condition may not be optimal for stable system operation at several lean–rich cycles. The balance for NH_3 is not kept and the value of θ_{NH_3} (the ratio between adsorbed NH_3 to catalyst NH_3 capacity) does not return to the initial value after lean–rich cycle (0.30 instead of 0.25) (Fig. 7A). This is because the SCR activity at lean mode is lower than the NO storage reduction activity. As a result, a higher amount of NO desorbed and reduced to ammonia at rich mode at the NOx storage unit than the reacted ammonia at lean mode on the SCR. Thus, the amount of adsorbed ammonia increases after each lean–rich cycle, i.e. θ_{NH_3}, does not return to the initial value and increases with every cycle. The SCR unit becomes saturated with ammonia increasing the slip. In this case, the two-unit system operates under non-optimized conditions that do not provide stable lean–rich cycles.

The developed simulator of two-unit system provided a viable solution to double the SCR volume and to halve the NOx storage volume. It did not change the total two-unit system volume, but ensured the balance between reacted and adsorbed NH_3 (Fig. 7B). Increasing the NH_3-SCR volume increased the NO conversion in the SCR, thus enhancing the amount of ammonia reacting with NO in the SCR. This balanced the amount of ammonia that reacted with NO at the SCR unit during the lean mode with the ammonia formed during the rich mode in the NOx storage and adsorbed in the SCR, ensuring stable operation of the two units.

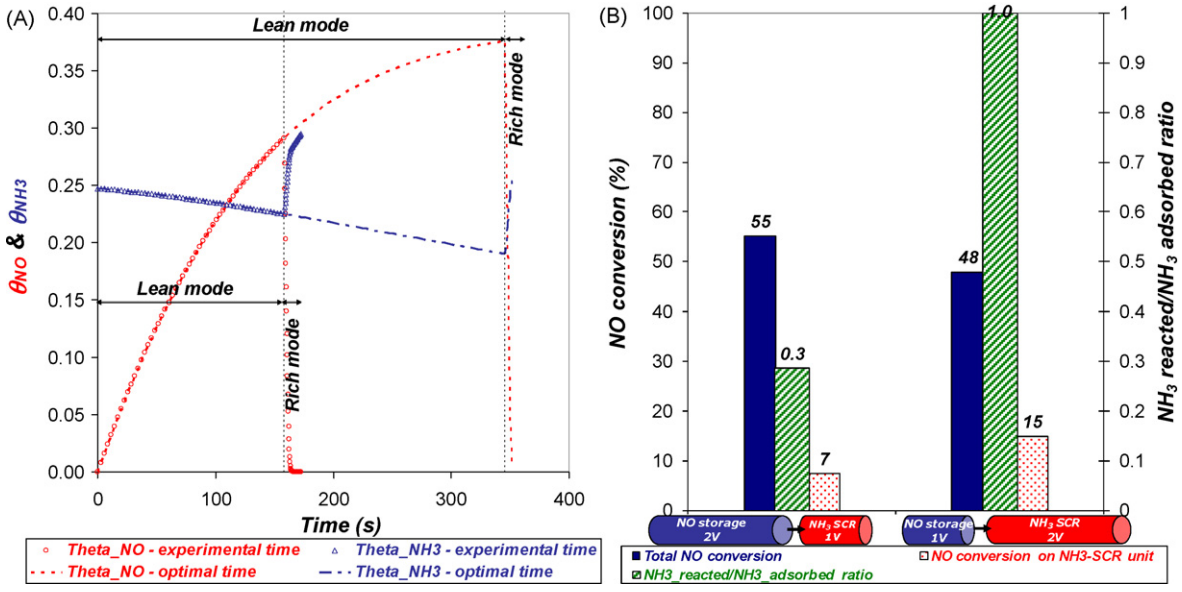

Fig. 7. (A) θ_{NO} and θ_{NH_3} (the ratio between adsorbed NO and NH_3 to catalyst capacity, respectively) in NOx storage unit and NH_3-SCR unit at EC1 condition, as function of time (at experimental time and at optimal time). (B) NO conversion and the ratio between reacted NH_3 and adsorbed (stored) NH_3 for two volume configurations at EC1 condition.

Another solution to achieve a stable lean–rich cycles is to modify the lean or/and rich period to the optimal values obtained from the simulator. For EC1, increasing the lean period (345 s instead of 165 s, Fig. 7A) enhances the amount of ammonia reacted in the SCR unit thus keeping the required ammonia balance. This example illustrates the simple control approach of this complicated smart catalytic converter that is based on changing the lean/rich duration for each operation condition using the developed simulator.

4. Conclusions

The development of the smart catalytic converter that relies on intrinsic dynamic operation and synchronization of several units requires detailed modeling and simulations. A simulator that predicts the dynamic behavior of several connected units in the aftertreatment system was developed. In addition, kinetic models were developed for NOx storage and NH_3-SCR unit, separately. The kinetic model for NOx storage also considers ammonia formation and oxidation in rich mode. Both kinetic models yielded good agreement with experimental data and were used in the integrated system simulation. The performance of the two-unit integrated system was simulated on the COMSOL package. The key factor for the aftertreatment system stability and control is the balance between stored and reacted NOx and ammonia in the NOx storage and SCR units. It was shown that the simulator is useful for optimization of lean and rich periods in order to ensure stable lean–rich cycles.

Acknowledgment

This work was supported by the European Commission in the Fifth Framework Programme under AHEDAT project, the contract #G3RD-CT-2002-00792.

References

[1] A. Koenig, W. Held, T. Richter, Lean-burn catalysts from the perspective of a car manufacturer. Early work at Volkswagen Research, Top. Catal. 28 (2004) 99–103.
[2] H. Bosch, F. Janssen, Catalytic reduction of nitrogen oxides. A review on the fundamentals and technology, Catal. Today 2 (1988) 369–521.
[3] P. Eastwood, Critical Topics in Exhaust Gas Aftertreatment, 1st ed., Research Studies Press Ltd., Baldock, England, 2000.
[4] T.J. Truex, R.A. Searles, D.C. Sun, Catalysts for nitrogen oxides control under lean burn conditions, Platinum Met. Rev. 36 (1992) 2–11.
[5] J. Kaspar, P. Fornasiero, N. Hickey, Automotive catalytic converters: current status and some perspectives, Catal. Today 77 (2003) 419–449.
[6] J.N. Armor, Catalytic removal of nitrogen oxides: where are the opportunities? Catal. Today 26 (1995) 99–105.
[7] N. Takahashi, H. Shinjoh, T. Iijima, T. Suzuki, K. Yamazaki, K. Yokota, H. Suzuki, N. Miyoshi, S.-i. Matsumoto, et al., The new concept 3-way catalyst for automotive lean-burn engine: NOx storage and reduction catalyst, Catal. Today 27 (1996) 63–69.
[8] M.A. Gomez-Garcia, V. Pitchon, A. Kiennemann, Pollution by nitrogen oxides. An approach to NOx abatement by using sorbing catalytic materials, Environ. Int. 31 (2005) 445–467.
[9] S.-W. Ham, I.-S. Nam, Selective catalytic reduction of nitrogen oxides by ammonia, Catalysis 16 (2002) 236–271.
[10] P. Forzatti, Present status and perspectives in de-NOx SCR catalysis, Appl. Catal., A 222 (2001) 221–236.
[11] P. Greening, European vehicle emission legislation—present and future, Top. Catal. 16/17 (2001) 5–13.
[12] A. Guethenke, D. Chatterjee, M. Weibel, B. Krutzsch, P. Koci, M. Marek, I. Nova, E. Tronconi, Current status of modeling lean exhaust gas aftertreatment catalysts, Adv. Chem. Eng. 33 (2008) 103–211.
[13] S.R. Katare, J.E. Patterson, P.M. Laing, Diesel aftertreatment modeling: a systems approach to NOx control, Ind. Eng. Chem. Res. 46 (2007) 2445–2454.
[14] S. Ogunwumi, R. Fox, M.D. Patil, L. He, In-situ NH3 generation for SCR NOx applications, Soc. Automot. Eng. SP-1723 (2002) 113–118.
[15] K. Vaezzadeh, C. Petit, V. Pitchon, A. Kiennemann, A new concept for the removal of NOx from a lean exhaust gas using storage on $H_3PW_{12}O_{40}{\cdot}6H_2O$, a very fast desorption and a reduction over a TWC, Catal. Commun. 3 (2002) 179–183.
[16] J.C. Wurzenberger, R. Wanker, Multi-scale SCR modeling, 1D kinetic analysis and 3D system simulation, Soc. Automot. Eng. SP-1940 (2005) 51–69.
[17] J. Guenther, B. Konrad, B. Krutzsch, A. Nolte, D. Voigtlaender, M. Weibel, M. Weirich, G. Wenninger, Exhaust gas Purification process and apparatus with internal generation of ammonia for reducing nitrogen oxide, US 6,338,244 B1 (January 15, 2002).
[18] P. Forzatti, L. Lietti, The reduction of NOx stored on LNT and combined LNT-SCR systems, Catal. Today, in press.
[19] G.C. Koltsakis, A.M. Stamatelos, Catalytic automotive exhaust aftertreatment, Prog. Energy Combust. Sci. 23 (1997) 1–39.
[20] C. Depcik, D. Assanis, One-dimensional automotive catalyst modeling, Prog. Energy Combust. Sci. 31 (2005) 308–369.
[21] J.H.B.J. Hoebink, J.M.A. Harmsen, M. Balenovic, A.C.P.M. Backx, J.C. Schouten, Automotive exhaust gas conversion: from elementary step kinetics to prediction of emission dynamics, Top. Catal. 16/17 (2001) 319–327.
[22] L.S. Mukadi, R.E. Hayes, Modelling the three-way catalytic converter with mechanistic kinetics using the Newton–Krylov method on a parallel computer, Comput. Chem. Eng. 26 (2002) 439–455.
[23] P. Koci, M. Kubicek, M. Marek, Periodic forcing of three-way catalyst with diffusion in the washcoat, Catal. Today 98 (2004) 345–355.
[24] D. Chatterjee, O. Deutschmann, J. Warnatz, Detailed surface reaction mechanism in a three-way catalyst, Faraday Discuss. 119 (2001) 371–384.
[25] S.E. Voltz, C.R. Morgan, D. Liederman, S.M. Jacob, Kinetic study of carbon monoxide and propylene oxidation on platinum catalysis, Ind. Eng. Chem. Prod. Res. Dev. 12 (1973) 294–301.
[26] S.H. Oh, J.C. Cavendish, Transients of monolithic catalytic converters. Response to step changes in feedstream temperature as related to controlling automobile emissions, Ind. Eng. Chem. Prod. Res. Dev. 21 (1982) 29–37.
[27] D.N. Tsinoglou, M. Weilenmann, A simplified three-way catalyst model for transient hot-mode driving cycles, Ind. Eng. Chem. Res. 48 (2009) 1772–1785.
[28] C. Dubien, D. Schweich, G. Mabilon, B. Martin, M. Prigent, Three-way catalytic converter modeling: fast- and slow-oxidizing hydrocarbons, inhibiting species, and steam-reforming reaction, Chem. Eng. Sci 53 (1997) 471–481.
[29] R.H. Heck, J. Wei, J.R. Katzer, Mathematical modeling of monolithic catalysts, AIChE J. 22 (1976) 477–484.
[30] S. Siemund, J.P. Leclerc, D. Schweich, M. Prigent, F. Castagna, Three-way monolithic converter: simulations versus experiments, Chem. Eng. Sci. 51 (1996) 3709–3720.
[31] S.-T. Lee, R. Aris, On the effects of radiative heat transfer in monoliths, Chem. Eng. Sci. 32 (1977) 827–837.
[32] T. Kirchner, G. Eigenberger, On the dynamic behavior of automotive catalysts, Catal. Today 38 (1997) 3–12.
[33] J. Jirat, F. Stepanek, M. Kubicek, M. Marek, Nonstationary operation of a system of catalytic monolithic reactors for selective NOx reduction, Chem. Eng. Sci. 54 (1999) 2609–2618.
[34] T. Shamim, H. Shen, S. Sengupta, S. Son, A.A. Adamczyk, A comprehensive model to predict three-way catalytic converter performance, J. Eng. Gas Turb. Power 124 (2002) 421–428.
[35] S. Tischer, O. Deutschmann, Recent advances in numerical modeling of catalytic monolith reactors, Catal. Today 105 (2005) 407–413.
[36] R. Holder, M. Bollig, D.R. Anderson, J.K. Hochmuth, A discussion on transport phenomena and three-way kinetics of monolithic converters, Chem. Eng. Sci. 61 (2006) 8010–8027.
[37] R.E. Hayes, S.T. Kolaczkowski, W.J. Thomas, Finite-element model for a catalytic monolith reactor, Comput. Chem. Eng. 16 (1992) 645–657.
[38] G. Groppi, A. Belloli, E. Tronconi, P. Forzatti, A comparison of lumped and distributed models of monolith catalytic combustors, Chem. Eng. Sci. 50 (1995) 2705–2715.
[39] R. Jahn, D. Snita, M. Kubicek, M. Marek, 3-D modeling of monolith reactors, Catal. Today 38 (1997) 39–46.
[40] R. Wanker, H. Raupenstrauch, G. Staudinger, A fully distributed model for the simulation of a catalytic combustor, Chem. Eng. Sci. 55 (2000) 4709–4718.
[41] A. Guethenke, D. Chatterjee, M. Weibel, N. Waldbuber, P. Koci, M. Marek, M. Kubicek, Development and application of a model for a NOx storage and reduction catalyst, Chem. Eng. Sci. 62 (2007) 5357–5363.
[42] F.X. Moser, Advanced heavy duty engine aftertreatment technology (AHEDAT). http://cordis.europa.eu/data/PROJ_FP5/ACTIONeqDndSESSIONeq-112242005919ndDOCeq111ndTBLeqEN_PROJ.htm (10/06/2009).
[43] U. Ullah, S.P. Waldram, C.J. Bennett, T. Truex, Monolithic reactors: mass transfer measurements under reacting conditions, Chem. Eng. Sci. 47 (1992) 2413–2418.
[44] J. Votruba, J. Sinkule, V. Hlavacek, J. Skrivanek, Heat and mass transfer in monolithic honeycomb catalysts, Chem. Eng. Sci. 30 (1975) 117–123.
[45] J.F. Brilhac, A. Sultana, P. Gilot, J.A. Martens, Adsorption, Pressure swing desorption of NOx in Na-Y Zeolite: experiments and modeling, Environ. Sci. Technol. 36 (2002) 1136–1140.
[46] M. Labaki, M. Mokhtari, J.F. Brilhac, S. Thomas, V. Pitchon, Simulation of NO and NO2 sorption-desorption-reduction behaviors on Pt-impregnated HPW supported on TiO_2, Appl. Catal., B 76 (2007) 386–394.
[47] A. Obuchi, S. Naito, T. Onishi, K. Tamaru, Mechanism of catalytic reduction of nitrogen monoxide by molecular hydrogen or carbon monoxide on a palladium foil; role of chemisorbed nitrogen on palladium, Surf. Sci. 122 (1982) 235–255.
[48] M.Y. Smirnov, D. Zemlyanov, Reactions of NH_2 Species with hydrogen and NO on the Pt(1 0 0)-(1*1) surface, J. Phys. Chem. B 104 (2000) 4661–4666.
[49] H. Hirano, T. Yamada, K.I. Tanaka, J. Siera, P. Cobden, B.E. Nieuwenhuys, Mechanisms of the various nitric oxide reduction reactions on a platinum-rhodium (1 0 0) alloy single crystal surface, Surf. Sci. 262 (1992) 97–112.
[50] J.L. Gland, V.N. Korchak, Ammonia oxidation on a stepped platinum single-crystal surface, J. Catal. 53 (1978) 9–23.

[51] C. Ciardelli, I. Nova, E. Tronconi, B. Konrad, D. Chatterjee, K. Ecke, M. Weibel, SCR-DeNOx for diesel engine exhaust aftertreatment: unsteady-state kinetic study and monolith reactor modelling, Chem. Eng. Sci. 59 (2004) 5301.
[52] G. Ramis, G. Busca, F. Bregani, P. Forzatti, Fourier transform-infrared study of the adsorption and coadsorption of nitric oxide, nitrogen dioxide and ammonia on vanadia-titania and mechanism of selective catalytic reduction, Appl. Catal. 64 (1990) 259–278.
[53] G. Ramis, G. Busca, C. Cristiani, L. Lietti, P. Forzatti, F. Bregani, Characterization of tungsta-titania catalysts, Langmuir 8 (1992) 1744–1749.
[54] G. Madia, M. Koebel, M. Elsener, A. Wokaun, Side reactions in the selective catalytic reduction of NOx with various NO_2 fractions, Ind. Eng. Chem. Res. 41 (2002) 4008–4015.